Geophysical Research Letters

RESEARCH LETTER
10.1029/2018GL078382

Estimating the Decoupling Degree of Subtropical Marine Stratocumulus Decks From Satellite

Youtong Zheng[1], Daniel Rosenfeld[2], and Zhanqing Li[1]

[1]Earth System Science Interdisciplinary Center, University of Maryland, College Park, MD, USA, [2]Institute of Earth Sciences, The Hebrew University of Jerusalem, Jerusalem, Israel

Key Points:
- A new satellite-based method for inferring the decoupling degree of Sc decks over subtropical oceans is proposed
- This method is based on an empirically found relationship between the decoupling degree and the satellite-derived skewness of liquid water path
- This method is not expected to be valid in regions where clouds are decoupled due to low-level warm advection to colder waters

Supporting Information:
- Supporting Information S1

Correspondence to:
Y. Zheng,
zhengyoutong@gmail.com

Citation:
Zheng, Y., Rosenfeld, D., & Li, Z. (2018). Estimating the decoupling degree of subtropical marine stratocumulus decks from satellite. *Geophysical Research Letters*, *45*, 12,560–12,568. https://doi.org/10.1029/2018GL078382

Received 20 APR 2018
Accepted 16 JUL 2018
Accepted article online 23 JUL 2018
Published online 20 NOV 2018

Abstracts The decoupling degree of stratocumulus (Sc) decks is an important quantity dictating evolutions of Sc. In subtropical oceans, the Sc decoupling is a key intermediate process of the Sc-to-cumulus transitions, a persistent phenomenon that is not fully understood. This study introduces a new approach for estimating the degree of decoupling of subtropical Sc decks using passive satellite sensors. This method is limited to regions where Sc decks are advected over progressively warmer water. This is most common in the subtropics. The estimation concept is that decoupled Sc clouds under cold-advection conditions are fed by spreading of the tops of cumulus clouds that are coupled. The cumulus clouds constitute a much larger liquid water path over small areas, which is identified by a positive skewness of the liquid water path, a quantity measurable from high-resolution satellite data. The decoupling degree here is defined as the difference between the Sc cloud-base height and lifting condensation level that is the cumulus cloud-base height under cold-advection conditions. This concept and the satellite-based estimations are supported by ship measurements over the Northeast Pacific. One-year climatology of the satellite-inferred decoupling degree was generated over the same region, revealing a coherent pattern of offshore decoupling, consistent with previous theory and field-campaign observations.

Plain Language Summary Our climate system is considerably sensitive to marine low clouds that reflect a great amount of incoming solar radiation and cool the earth. These marine clouds are intimately coupled with the underlying sea surfaces that feed moisture and energy to the clouds for sustaining them. The degree of the surface-cloud coupling (SCC) considerably influences the cloud properties, which in turn modulates the temperature of our climate system. Despite its significance to climate, the SCC degree has never been measured from satellite, the only observational tool that offers global coverage. This study addresses this long-lasting issue by developing an innovative method to estimate the SCC degree using satellite data. The validity of this method is demonstrated by validating the SCC degree estimated by this new method against *ground truth* measurements over the Northeast Pacific. This method offers unprecedentedly new geophysical information, namely, the SCC degree that is crucial for the understanding of behavior of marine low clouds and its interactions with our climate system. This will eventually improve the accuracy with which future climate change is projected.

1. Introduction

Marine stratocumulus (Sc) is the most extensive and reflective cloud type, to which the climate system is sensitive (Hartmann et al., 1992; Stephens, 2005). They often occur, in a layer form, at the top of marine boundary layers (MBL) in which radiatively driven convective circulation well mixes the MBL and couples the clouds with the surface (Lilly, 1968; Wood, 2012; Zheng et al., 2016). The system is characterized by a vertically uniform distribution of moist-conserved quantities (e.g., equivalent potential temperature and total water mixing ratio) from the surface to the capping inversion bottom. The decoupling of the coupled surface-Sc system is a process by which the Sc decks are separated from the surface. The decoupling features a stratification of moist-conserved quantities, leading to a two-layer structure of MBL: a radiatively driven Sc-containing layer and a surface mixed layer. These two layers, each of which is well mixed, are separated by a stable layer. The decoupling could be driven by a number of factors that fall into two categories: (1) those reducing the proportional strength of radiatively driven turbulence relative to a certain depth of MBL and (2) those stabilizing the subcloud layer. The former is exemplified by the daytime insolation that heats the cloud layer and reduces the cloud-top radiative cooling to the extent that the generated turbulence is no longer vigorous enough for maintaining a well-mixed MBL. Similarly, if a Sc-capped MBL is deepened, usually by entrainment of free-tropospheric air, to an extent that even the strongest radiatively driven turbulence cannot mix through such a deep MBL, decoupling occurs (Bretherton & Wyant, 1997). The second decoupling regime is associated with the stabilization of subcloud layer. Processes such as precipitation (Nicholls, 1984) and horizontal warm temperature advection (Stevens et al., 1998) could induce such stabilization and decoupling.

The decoupling degree of Sc decks has been considered as an important quantity dictating evolutions of Sc decks. In subtropical oceans, the decoupling marks the first stage for the transitions of coastal overcast Sc decks to downstream cumulus (Cu) clouds, a robust pattern of cloud climatology that fuels a large number of studies during the past decades (e.g., Albrecht et al., 1995; Bretherton & Wyant, 1997; Sandu & Stevens, 2011; Stevens, 2000). The decoupling observations are mostly limited to ship- or aircraft-borne measurements (Albrecht et al., 1995; Jones et al., 2011; Zuidema et al., 2009). Satellite observations remain scant. The first attempt was made by Wood and Bretherton (2004) who estimate the decoupling degree of Sc-topped MBLs by assuming a certain MBL structure. Their estimations, however, lack systematic ground-based validations. In addition, their methodology relies heavily on reanalysis data (six out of nine inputs are from reanalysis) and therefore may not be considered as a satellite-based approach but a simple model that ingests satellite data as part of the input. With the presence of active satellite sensors, Luo et al. (2016) use the aerosol lidar backscattering from Cloud-Aerosol Lidar and Infrared Pathfinder Satellite Observations to infer the MBL top and the height of surface mixing layer, which combined to offer the decoupling degree of MBL. Their method, however, only works for cloud-free MBLs, whereas cloudy MBLs are of most interest. Also, a narrow swath of the Cloud-Aerosol Lidar and Infrared Pathfinder Satellite Observations considerably limits its spatial coverage.

In this study, we introduce a new approach for estimating the degree of decoupling of Sc decks using passive satellite sensor data. This method is limited to regions where Sc decks are advected over progressively warmer sea surfaces, as typical to the subtropics. The only input for this method is the skewness of liquid water path (LWP). The concept for this method will be elaborated in the next section, followed by a case study and statistical analysis from the Marine Atmospheric Radiation Measurement (ARM) Global Energy and Water Cycle Experiment-Cloud System Study-Pacific Cross-section Intercomparison Investigation of Clouds (MAGIC) field campaign (Lewis & Teixeira, 2015) to illustrate its utility. A year-long climatology of the satellite-inferred decoupling degree of Sc decks over the Northeast Pacific will be presented to demonstrate the robustness of this method. Finally, we will discuss the applicability of this method to other regions, followed by a conclusion.

2. The Estimation Concept

The estimation concept is illustrated in Figure 1. In a well-mixed MBL (Figure 1a), the LWP follows a normal distribution (Wood & Hartmann, 2006). When the Sc decks become decoupled, a thermodynamic stratification occurs, which detaches the bases of Sc deck from the surface mixed layer whose depth is approximated by the lifting condensation level (LCL; red dashed lines). Under conditions of cold advection, such as in subtropics, such a two-layer structure of decoupling is unsteady. The progressively warmed sea surface offers thermodynamic settings conducive for the formation of Cu clouds that penetrate through the weakly stable layer, feeding moisture to the previously decoupled Sc decks (Figure 1b). These geometrically thicker Cu clouds contain more liquid water, rendering the probability density function (PDF) of LWP positively skewed (Figure 1b). Note that such a Cu-fed Sc regime, as a whole, could still be considered as coupled with the surfaces due to the Cu feeding (Martin et al., 1995; M. A. Miller & Albrecht, 1995). Such a cloud-surface coupling, however, is intermittent and local, and its strength is markedly weaker than that in well-mixed MBLs (Zheng et al., 2018). In the context of this study, we consider the decoupling degree as a system-wide integrated quantity. In this sense, while Cu clouds locally couple a certain fraction of the Sc system, the vast majority of the Sc decks still remain decoupled. As the MBL further deepens, Sc decks become increasingly decoupled from the surface (Bretherton & Wyant, 1997; Wood & Bretherton, 2004). This leads to deeper Cu clouds with larger LWP that feed the Sc decks, thus further skewing the LWP PDF (Figure 1c).

Such an increase in LWP skewness with decoupling degree of Sc decks should be a gradual process. The decoupling degree could be quantified as the difference between the Sc base height (z_{b_sc}) and LCL height (z_{LCL}). The larger the difference is, the fewer and the deeper the Cu clouds are, and the more skewed the PDF of LWP is. Thus, the spectrum of the decoupling degree should match the spectrum of LWP skewness to a certain extent. One extreme situation is a deep MBL capped by strongly decoupled Sc where only a small

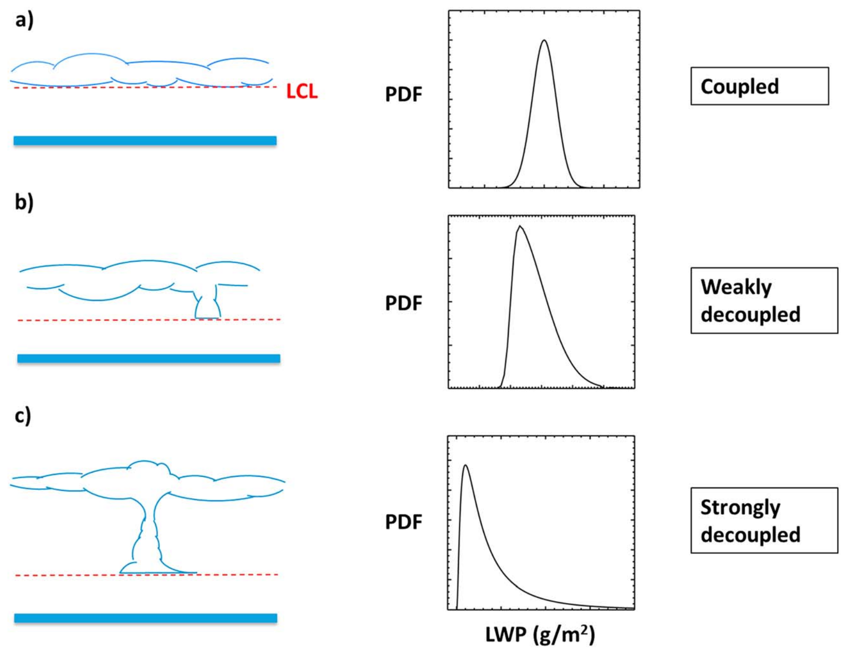

Figure 1. Cartoons illustrating the linkages between the decoupling degree of stratocumulus decks and the skewness of LWP PDF for (a) coupled, (b) weakly coupled, and (c) strongly decoupled marine boundary layers. The dashed red lines mark the LCL. LCL = lifting condensation level; LWP = liquid water path; PDF = probability density function.

population of deep cloud elements feeds the thin Sc anvils. The cumuli could be so vigorous to break up the Sc decks through efficient entrainment drying. Thin Sc anvils will be dissipated faster than the deep cloud elements, and thus, the LWP skewness should still remain large. Therefore, the decoupling-skewness relationship could hold even after the Sc decks start to break up. The relationship ceases when the Sc anvils are mostly dissipated and cumuliform clouds become dominant.

3. Data and Methodology

3.1. Data

We use 6-month-long ship observations (2012–2013) made during the MAGIC field campaign. A commercial ship Horizon *Spirit* that carries U.S. Department of Energy ARM Program Mobile Facility 2 instruments made round trips between Los Angeles, California, and Honolulu, Hawaii. Cloud base heights were measured from a ship-borne ceilometer. A Ka-band ARM Zenith Radar (KAZR), which detects hydrometeors in the atmospheric column, was used to characterize cloud boundaries and their evolutions. Vertical structures of MBL thermodynamics are from radiosondes launched four times per day. Inversion base height (z_i) were determined by finding the altitude where the temperature inversion is the strongest below 3 km. Standard surface meteorological measurements include the near-surface air temperature and relative humidity, which are used to compute the z_{LCL} based on Epsy's formula (Bohren & Albrecht, 1998).

Two sets of satellite LWP data sets are used: the Fifteenth Geostationary Operational Environmental Satellite (GOES-15) cloud product generated by National Aeronautics and Space Administration Langley center and the Aqua MODerate-resolution Imaging Spectroradiometer (MODIS) level-2 cloud optical and microphysical product (Platnick et al., 2017). The spatial resolutions are 4 and 1 km for GOES-15 and MODIS, respectively. LWP is calculated as LWP = $\frac{5}{9}\rho_w r_e \tau$, where ρ_w, r_e, and τ represent the liquid water density, cloud effective radius at 3.7 μm, and cloud optical depth, respectively. A weakness of the LWP derived by this bispectral solar reflectance method is that the pixel-level LWP estimate becomes biased when a cloud field becomes more cumuliform-like (Lebsock & Su, 2014; D. J. Miller et al., 2016). However, the relative error from pixel to pixel, which plays a more important role in influencing the skewness, is likely to be much smaller.

3.2. Decoupling Measure

We use the difference between ceilometer-measured z_{b_sc} and z_{LCL} as a metric for decoupling:

$$\Delta z_{sc} = \overline{z_{b\_sc} - z_{LCL}},$$

where the overbar represents an average over a group of samples. This metric has been widely used to quantify the decoupling degree of subtropical Sc decks (Jones et al., 2011; Zheng et al., 2016; Zhou et al., 2015). The limitation of this metric is that it becomes less valid when the cloud fraction (CF) reduces to the degree that the ground-based samplings are no longer representative of the entire broken cloud fields. To overcome this limitation, McGibbon and Bretherton (2017) found that Sc cloud base, if present, could be well approximated by the LCL calculated using thermodynamic quantities at the height of $0.7z_i$, which is denoted as ${z_{LCL}}^{0.7zi}$. This quantity, however, is only available during the times of sounding and may incur additional uncertainties due to sampling limitations of single-point radiosondes. To reconcile the respective limitations, we use the ${z_{LCL}}^{0.7zi}$ to calculate the Δz_{sc} only when a full spectrum of CF is considered. In other conditions with CF $>$ 50%, which is the main focus of this study, we keep using the original metric.

This study is targeted at stratiform Sc decks, but, as was discussed; decoupled Sc decks often coexist with Cu clouds underneath them. These Cu are hypothesized to be coupled (Figure 1). To test this hypothesis, we quantify the coupling state of the underlying Cu by comparing the cloud-base heights of Cu clouds (z_{b_cu}) to the z_{LCL}. Here we use the lowest 5% of ceilometer-measured cloud base heights in a time window of ship measurements (e.g., 3 hr) to approximate the z_{b_cu}. The coupling state of the Cu clouds is thus defined as:

$$\Delta z_{cu} = z_{b\_cu} - \overline{z_{LCL}}.$$

4. Results

4.1. A Case Study

We start with a case study to illustrate the underlying mechanism of Sc decoupling process and how it is related to LWP skewness. Figure 2a shows a height-time image of KAZR radar profiling vertical structures of Sc decks along the track of the *Spirit* ship from 20 universal time coordinated, 3 August to 24 universal time coordinated, 5 August 2013. During this period, the ship moved offshore from near-coastal regions. Segments of daytime/night are marked by the white/gray shadings in Figure 2h. At the beginning, the Sc decks were coupled with the surfaces as seen from a close match between ceilometer-measured cloud bases (black points) and LCL (red points). The corresponding GOES scenes of LWP (Figures 2b and 2c) show extensive cloud sheets with certain degrees of cellular feature. At around 15 hr, decoupling starts to occur as seen from a gradual diverge of cloud bases from the LCL. In the meantime, Cu clouds emerge. They extend from the LCL to the bases of the decoupled Sc decks and penetrate into the capping inversion, elevating the cloud tops relative to the surroundings and increasing precipitation as indicated by columns of large values of KAZR backscatter (marked by the red arrows). Such a feature of Cu-fed Sc regimes is visible from the satellite scene (Figure 2d) that presents distinct cellular patterns: groups of high-LWP cloud cells surrounded by low-LWP ones. Six hours later, the insolation-induced reduction of convection accumulates to the extent that the Sc decks become considerably thinner, as seen from the radar image at ~30 hr. This behavior is also reflected in the satellite image (Figure 2e) showing considerably lower values of LWP and smaller Cu-feeding regions (LWP $>$ 300 g/m^2) than 6 hr ago. As the nighttime comes, the cloud top radiative cooling strengthens. On one hand, the enhanced convection increases the moisture supply via allowing more Cu clouds to develop for feeding the Sc decks. This is indicated by the radar image showing a more frequent occurrence of precipitation and also by the satellite image in the next morning (Figure 2f) showing larger fraction of clouds with high LWP values. On the other hand, the strong convection facilitates cloud-top entrainment, leading to a much deepened and more decoupled MBL. This eventually breaks up the Sc decks (Figure 2g).

The entire decoupling process is accompanied with an overall trend of increased ship-measured decoupling degree Δz_{sc} (black lines in Figure 2h) and increased skewness of GOES-derived LWP (S_{LWP}, blue line in Figure 2h). Although the S_{LWP} decreases after the Sc decks start to break up (after ~50 hr), which is not a common behavior as will be seen later, the value of S_{LWP} still remains large relative to the coupled Sc.

4.2. Statistical Analysis

Figure 3a shows the S_{LWP}, Δz_{sc}, and Δz_{cu} versus GOES-derived CF for a total of 151 selected cases (see supporting information S1 for case selection). Each case represents a 3-hr segment of ship observations.

10.1029/2018GL078382

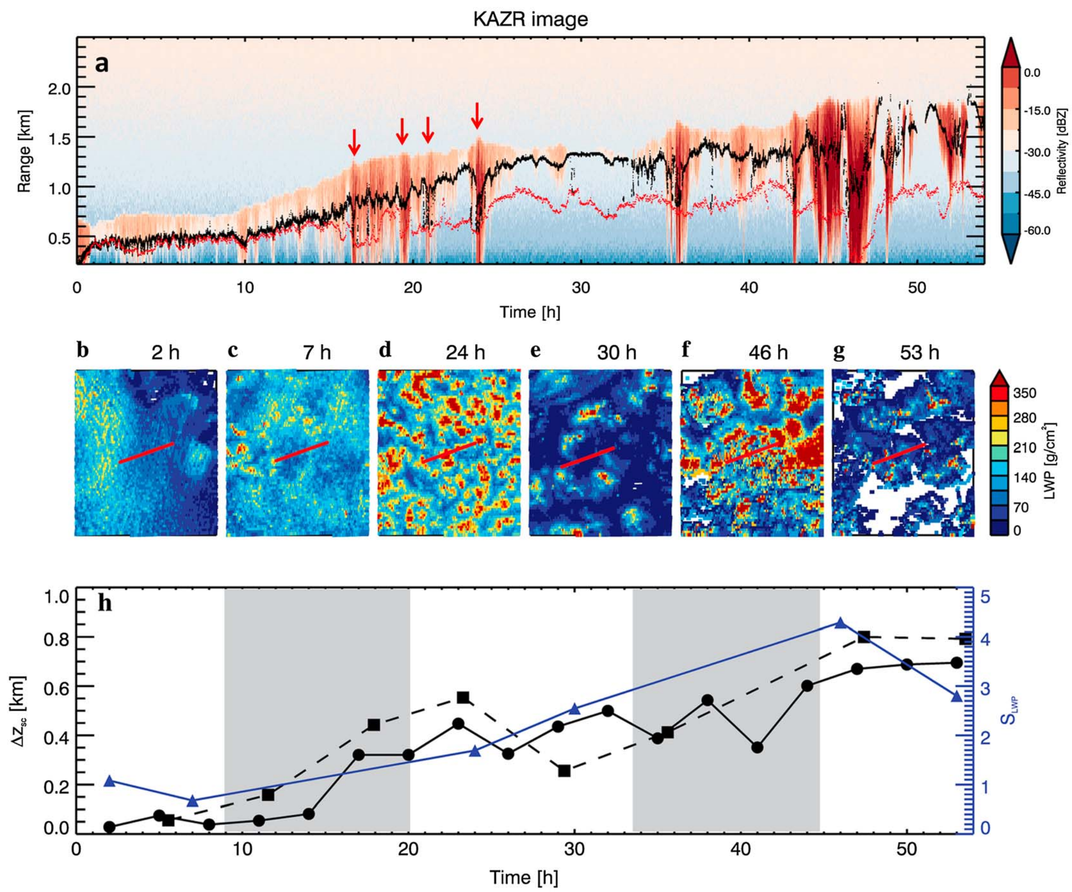

Figure 2. An example case of stratocumulus decks becoming decoupled. (a) Height-time plot of KAZR radar reflectivity starting at 20 universal time coordinated on 3 August and ending at 24 universal time coordinated on 5 August 2013. The black and red points mark the ceilometer-measured cloud-base height and calculated lifting condensation level, respectively. (b)–(g) show the 3 × 3° scenes of Geostationary Operational Environmental Satellite-derived LWP centered on ship locations at times indicated at the top of each figure. The 3-hr ship tracks are marked by thick red lines. (h) Temporal variations of $\overline{z_{\mathrm{bsc}} - z_{\mathrm{LCL}}}$ (solid black), $\overline{z_{\mathrm{LCL}}{}^{0.7zi} - z_{\mathrm{LCL}}}$, (dashed black), and skewness of LWP (solid blue) for 1.5 × 1.5° areas centered on ship locations. The white and gray shadings mark the segments of daytime and nighttime, respectively. KAZR = Ka-band Atmospheric Radiation Measurement Zenith Radar; LWP = liquid water path.

First of all, the Δz_{cu} (open blue rectangles) retains low values across the full spectrum of CF, indicating a ubiquitous presence of Cu clouds that are tightly coupled with the surface. We also plot, in the upper panel of Figure 3a, the ceilometer-measured CF of the coupled cloud bases (black bars) and its ratio (blue solid line) over total CF (gray bars) during a 3-hr segment. The coupled-cloud CF is determined as the percentage of cloud measurements with $z_{\mathrm{b\_sc}} - z_{\mathrm{LCL}} < 0.2$ km. In overcast conditions, the coupled-cloud CF (blue line) is not high ($<$50%), which seems to be inconsistent with the intuition that a majority of clouds in overcast Sc should be coupled. This is because of the frequent occurrence of Cu-fed Sc (Klein & Hartmann, 1993) that often maintains extensive cloud cover despite the presence of highly decoupled Sc decks (Figure 1c). As the CF decreases, the coupled-cloud CF presents an overall decrease-then-increase trend. The initial decrease is associated with offshore decoupling. When decoupled Sc anvils dissipate, the coupled Cu clouds dominate, increasing the coupled-cloud CF.

In addition, the reduction of CF is accompanied with a marked increase in Δz_{sc}. This is consistent with the significant role of decoupling in breaking up the Sc decks. This trend ceases and remains flat after the CF decreases below ~50%. This threshold value corresponds to a typical CF value for open cells (Muhlbauer et al., 2014) in which these Sc are in fact the anvils. These anvils represent the most decoupled Sc. The S_{LWP} shares a similar trend: it first increases with decreasing CF in high-CF conditions, and the increase ceases after the CF drops below ~50%. As was discussed in section 2, the S_{LWP} as a predictor for the decoupling

10.1029/2018GL078382

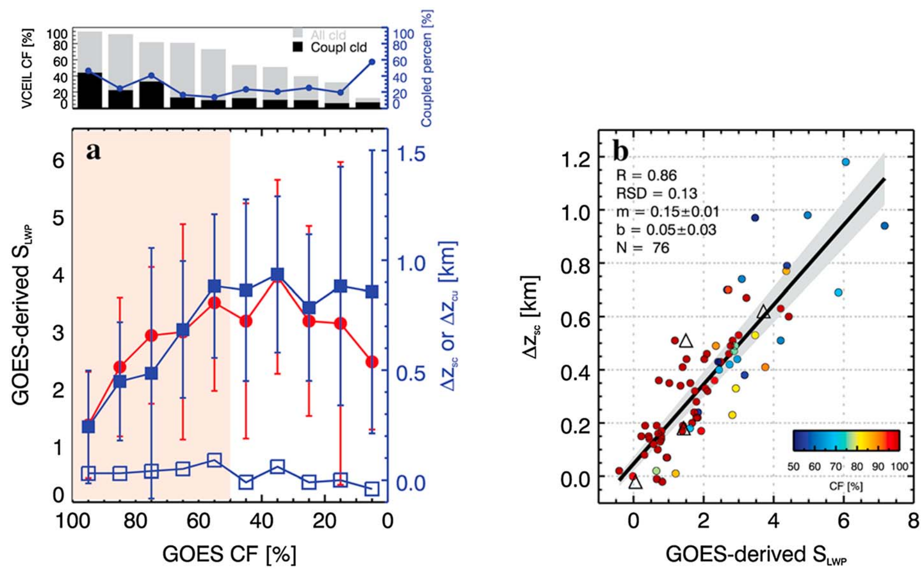

Figure 3. (a) Variations of GOES-derived S_{LWP} for 1.5° × 1.5° satellite scenes centered on ship locations (red solid circle), ship-measured Δz_{sc} (blue solid rectangle), and Δz_{cu} (blue open rectangle) with the CF. Error bars represent the standard deviations in each bin. We did not plot error bars of Δz_{cu} for clarity of presentation. The upper panel shows the ceilometer-measured CF of the coupled cloud bases (black bars) and its ratio (blue solid line) over total CF (gray bars) during a 3-hr segment. (b) Ship-measured Δz_{sc} versus GOES-derived S_{LWP} for cases with CF greater than 50%. Each case is color-coded by the CF. The open upward triangles mark the four MODerate-resolution Imaging Spectroradiometer cases. CF = cloud fraction; cu = cumulus; GOES = Geostationary Operational Environmental Satellite; LWP = liquid water path; sc = stratocumulus.

should cease to be skillful after the Sc breakup proceeds to a certain extent. Here the CF of ~50% seems to be an appropriate threshold. In addition, after the CF decreases below 50%, both the surface-derived Δz_{sc} and satellite-derived S_{LWP} become technically more uncertain. The former is because of the greater difficulty in identifying z_i in weak-inversion conditions (Jones et al., 2011), and the latter is due to the insufficient number of pixels for establishing statistically robust distributions and the known problems of LWP retrieval for highly broken clouds. In either case, Sc clouds with CF $>$ 50% are most relevant for investigating the S_{LWP}-Δz_{sc} in the context of this study. As such, cases with CF $>$ 50% were extracted for further analysis. A direct comparison between the S_{LWP} and Δz_{sc} shows a remarkably tight relationship with correlation coefficient (R) of 0.86, as shown in Figure 3b. The y-intercept value of the best-fit line is close to zero, consistent with the idea that a Sc that is fully coupled with the surface follows a nonskewed PDF. There is a slight dependence of the relationship on the size of satellite scene when we vary the domain size from 0.5° × 0.5° to 2.5° × 2.5° (Table S1), but the sensitivity is weak in particular when it is greater than 1° × 1°.

The statistically significant relationship makes S_{LWP} a useful predictor for the extent to which Cu occurs below the Sc and thus the decoupling degree of the overlying Sc decks. As a sanity check, we use the GOES-derived S_{LWP} to derive a 1-year climatology of the Sc decoupling degree over the Northeast Pacific Ocean (Figure 4) using the best-fit linear relationship, $\Delta z_{sc} = 0.15 \times S_{LWP} + 0.05$, from Figure 3a. The well-known pattern of systematic offshore decoupling is robustly captured: a progressively increased degree of decoupling from near-coastal regions equatorward to warm-sea surface temperature regions. This behavior is consistent with the *deepening-warming* decoupling mechanism by Bretherton and Wyant (1997).

5. Discussion of the Applicability: A Fortuitous Relationship or Not?

The encouraging results above lead to two practical questions: (1) How is this method applied to the other passive satellite sensors and (2) Is it applicable to other subtropical oceans? The first question is motivated by the fact that the resolution the GOES-15 LWP data is 4 km, at least fourfold coarser than high-resolution satellite sensors onboard polar-orbiting satellite platforms (e.g., MODIS and Visible Infrared Imaging Radiometer Suite) that can provide much larger coverage. Thus, we survey LWP retrievals from the Aqua

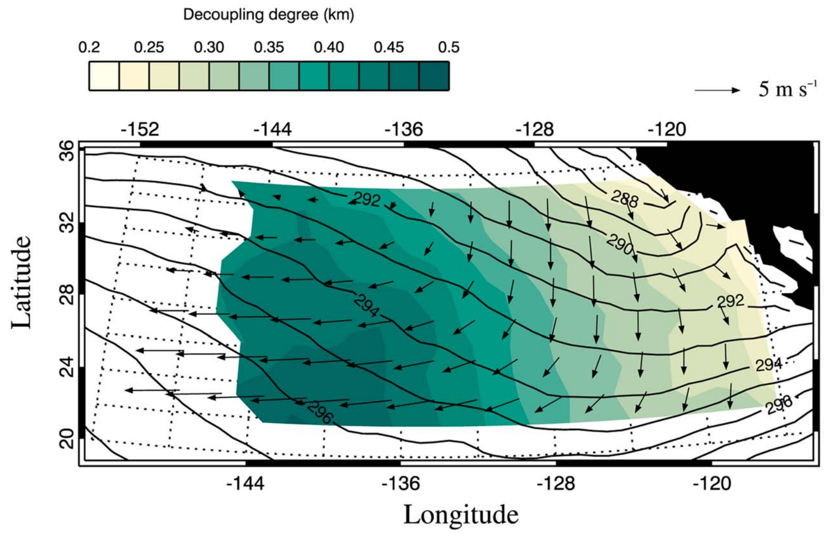

Figure 4. A climatology of the Geostationary Operational Environmental Satellite inferred Δz_{SC} over the Northeast Pacific from October 2012 to October 2013. The black contours and arrows mark the climatological sea surface temperature (unit: Kelvin degree) and wind vectors derived from European Center for Medium Range Weather Forecasts ERA-Interim reanalysis, respectively. Estimations of Δz_{SC} were only performed for regions with fraction of retrievals that meet criteria (solar zenith angle $<70°$ and CF $>$ 50%) greater than 10%.

MODIS cloud products (MYD06) with the horizontal resolution of ~1 km in nadir. The number of samples is significantly limited by the demand for a spatiotemporal match between the Aqua and the *Spirit* ship. There are only four such cases, which are superimposed (marked by open upward triangles) in Figure 3b. These cases well fit the relationship. The high-resolution data can resolve finer cloud elements, which could make difference to either direction of tail in a LWP PDF, but its combined effect on the skewness is much less marked. To examine this idea, we perform a simple sensitivity test by degrading the 1-km MODIS data to 2- and 4-km for two representative cases (an overcast closed cell and an open cell). Little sensitivity is noticed (Figures S1 and S2).

Regarding to the second question, there are two pieces of evidence supporting the potentially wide applicability of S_{LWP} as an effective decoupling predictor over subtropical oceans. First, the central physical mechanism, upon which this method is established, is the advection of Sc decks over progressively warmer water. This is a coherent phenomenology over subtropical oceans where equatorward advections of air toward warmer sea surface temperature are a dominant pattern (Klein & Hartmann, 1993; Wood, 2012). It has been suggested (Sandu et al., 2010; Wood & Hartmann, 2006) that the decoupling mechanisms and the resultant transition in cloudiness are shared by four major subtropical oceans.

Second, a key linkage in the chain that relates the S_{LWP} with the decoupling degree is the occurrence of Cu feeding. Such a Cu-feeding phenomenon has been extensively observed (e.g., Albrecht et al., 1995; Klein et al., 1995; Martin et al., 1995) and simulated by large-eddy simulations (e.g., McGibbon & Bretherton, 2017; Sandu & Stevens, 2011; Stevens, 2000; Wyant et al., 1997). Deeper Cu clouds in Cu-fed Sc regimes cause stronger precipitation. A distinct downstream increase in precipitation from the west coasts of the major continents, the same pattern with the offshore decoupling, has been identified by spaceborne radar onboard the CloudSat satellite as a robust precipitation climatology (Lebsock & L'Ecuyer, 2011; Wood et al., 2012). This indirectly supports the prevalent occurrences of Cu feeding regimes in subtropics.

6. Conclusion

A new satellite-based approach for inferring the decoupling degree of subtropical Sc decks is proposed. The only input quantity is the skewness of satellite-derived LWP (S_{LWP}) on a spatial scale of 100–200 km, which is intimately related with the decoupling degree. The concept for the inference is as follows: a more decoupled Sc deck allows for deeper but fewer Cu clouds that penetrate through weakly stable subcloud layers for feeding the Sc decks, leading to a more skewed distribution of LWP. Using ship-based measurements and GOES-derived LWP during the MAGIC field campaign over the Northeast Pacific, we have found a statistically significant linear relationship (R = 0.86) between the decoupling degree, defined by the difference between the mean cloud-base heights of Sc decks and LCL, and the GOES-derived S_{LWP} for clouds with fractional coverage greater than 50%. This simple relationship was applied for generating a 1-year climatology of satellite-inferred decoupling degree over the Northeast Pacific. The climatology captures a robust pattern of an increasing degree of decoupling away from the coast of continent, which is consistent with previous theory and observations from field campaigns. This method is limited to conditions where low-level warm temperature advection is absent because advection of clouds over colder water stabilizes the MBL and prevents Cu convection (Goren et al., 2018). In middle or high latitude, the frequent occurrence of warm temperature advection may considerably limit the application of this method. To justify this hypothesis, more extensive validations are still needed. We plan to pursue this in future work.

Acknowledgments

The study was supported by the NOAA's Joint Polar Satellite System (JPSS) program and National Weather Service (NWS) program (NA15NWS4680011) and Department of Energy (DOE) Atmospheric System Research program (DE-SC0018996). The second author is supported by the Joint NSFC-ISF Research Program (41561144004). The ground-based data are available from website of ARM Climate Research Facility (www.http://www.archive.arm.gov/data). The GOES-15 cloud parameters data are obtained from the NASA Langley Cloud and Radiation Research Group (satcorps.larc.nasa.gov). The MODIS data are available from LAADS Distributed Active Archive Center (ladsweb.modaps.eosdis.nasa.gov). The authors thank David Painemal for sharing the MODIS data although they are not eventually used in this study.

References

Albrecht, B. A., Bretherton, C. S., Johnson, D., Schubert, W. H., & Frisch, A. S. (1995). The Atlantic stratocumulus transition experiment—ASTEX. *Bulletin of the American Meteorological Society*, *76*(6), 889–904. https://doi.org/10.1175/1520-0477(1995)076<0889:TASTE>2.0.CO;2

Bohren, C. F., & Albrecht, B. A. (1998). *Atmospheric thermodynamics*. Oxford, UK: Oxford University Press.

Bretherton, C. S., & Wyant, M. C. (1997). Moisture transport, lower-tropospheric stability, and decoupling of cloud-topped boundary layers. *Journal of the Atmospheric Sciences*, *54*(1), 148–167. https://doi.org/10.1175/1520-0469(1997)054<0148:MTLTSA>2.0.CO;2

Goren, T., Rosenfeld, D., Sourdeval, O., & Quaas, J. (2018). Satellite observations of precipitating marine stratocumulus show greater cloud fraction for decoupled clouds in comparison to coupled clouds. *Geophysical Research Letters*, *45*(10), 5126–5134. https://doi.org/10.1029/2018GL078122

Hartmann, D. L., Ockert-Bell, M. E., & Michelsen, M. L. (1992). The effect of cloud type on Earth's energy balance: Global analysis. *Journal of Climate*, *5*(11), 1281–1304. https://doi.org/10.1175/1520-0442(1992)005<1281:TEOCTO>2.0.CO;2

Jones, C., Bretherton, C., & Leon, D. (2011). Coupled vs. decoupled boundary layers in VOCALS-REx. *Atmospheric Chemistry and Physics*, *11*(14), 7143–7153. https://doi.org/10.5194/acp-11-7143-2011

Klein, S. A., & Hartmann, D. L. (1993). The seasonal cycle of low stratiform clouds. *Journal of Climate*, *6*(8), 1587–1606. https://doi.org/10.1175/1520-0442(1993)006<1587:TSCOLS>2.0.CO;2

Klein, S. A., Hartmann, D. L., & Norris, J. R. (1995). On the relationships among low-cloud structure, sea surface temperature, and atmospheric circulation in the summertime Northeast Pacific. *Journal of Climate*, *8*(5), 1140–1155. https://doi.org/10.1175/1520-0442(1995)008<1140:OTRALC>2.0.CO;2

Lebsock, M., & Su, H. (2014). Application of active spaceborne remote sensing for understanding biases between passive cloud water path retrievals. *Journal of Geophysical Research: Atmospheres*, *119*, 8962–8979. https://doi.org/10.1002/2014JD021568

Lebsock, M. D., & L'Ecuyer, T. S. (2011). The retrieval of warm rain from CloudSat. *Journal of Geophysical Research*, *116*, D20209. https://doi.org/10.1029/2011JD016076

Lewis, E., & Teixeira, J. (2015). Dispelling clouds of uncertainty, *Eos. Transactions American Geophysical Union* (Online), *96*(BNL--107566-2015-JA).

Lilly, D. K. (1968). Models of cloud-topped mixed layers under a strong inversion. *Quarterly Journal of the Royal Meteorological Society*, *94*(401), 292–309. https://doi.org/10.1002/qj.49709440106

Luo, T., Wang, Z., Zhang, D., & Chen, B. (2016). Marine boundary layer structure as observed by A-train satellites. *Atmospheric Chemistry and Physics*, *16*(9), 5891–5903. https://doi.org/10.5194/acp-16-5891-2016

Martin, G., Johnson, D., Rogers, D., Jonas, P., Minnis, P., & Hegg, D. (1995). Observations of the interaction between cumulus clouds and warm stratocumulus clouds in the marine boundary layer during ASTEX. *Journal of the Atmospheric Sciences*, *52*(16), 2902–2922. https://doi.org/10.1175/1520-0469(1995)052<2902:OOTIBC>2.0.CO;2

McGibbon, J., & Bretherton, C. (2017). Skill of ship-following large-eddy simulations in reproducing MAGIC observations across the Northeast Pacific stratocumulus to cumulus transition region. *Journal of Advances in Modeling Earth Systems*, *9*, 810–831. https://doi.org/10.1002/2017MS000924

Miller, D. J., Zhang, Z., Ackerman, A. S., Platnick, S., & Baum, B. A. (2016). The impact of cloud vertical profile on liquid water path retrieval based on the bispectral method: A theoretical study based on large-eddy simulations of shallow marine boundary layer clouds. *Journal of Geophysical Research: Atmospheres*, *121*, 4122–4141. https://doi.org/10.1002/2015JD024322

Miller, M. A., & Albrecht, B. A. (1995). Surface-based observations of mesoscale cumulus–stratocumulus interaction during ASTEX. *Journal of the Atmospheric Sciences*, *52*(16), 2809–2826. https://doi.org/10.1175/1520-0469(1995)052<2809:SBOOMC>2.0.CO;2

Muhlbauer, A., McCoy, I. L., & Wood, R. (2014). Climatology of stratocumulus cloud morphologies: Microphysical properties and radiative effects. *Atmospheric Chemistry and Physics*, *14*(13), 6695–6716. https://doi.org/10.5194/acp-14-6695-2014

Nicholls, S. (1984). The dynamics of stratocumulus: Aircraft observations and comparisons with a mixed layer model. *Quarterly Journal of the Royal Meteorological Society*, *110*(466), 783–820. https://doi.org/10.1002/qj.49711046603

Platnick, S., Meyer, K. G., King, M. D., Wind, G., Amarasinghe, N., Marchant, B., et al. (2017). The MODIS cloud optical and microphysical products: Collection 6 updates and examples from Terra and Aqua. *IEEE Transactions on Geoscience and Remote Sensing*, *55*(1), 502–525. https://doi.org/10.1109/TGRS.2016.2610522

Sandu, I., & Stevens, B. (2011). On the factors modulating the stratocumulus to cumulus transitions. *Journal of the Atmospheric Sciences*, *68*(9), 1865–1881. https://doi.org/10.1175/2011JAS3614.1

Sandu, I., Stevens, B., & Pincus, R. (2010). On the transitions in marine boundary layer cloudiness. *Atmospheric Chemistry and Physics*, *10*(5), 2377–2391. https://doi.org/10.5194/acp-10-2377-2010

Stephens, G. L. (2005). Cloud feedbacks in the climate system: A critical review. *Journal of Climate*, *18*(2), 237–273. https://doi.org/10.1175/JCLI-3243.1

Stevens, B. (2000). Cloud transitions and decoupling in shear-free stratocumulus-topped boundary layers. *Geophysical Research Letters*, *27*(16), 2557–2560. https://doi.org/10.1029/1999GL011257

Stevens, B., Cotton, W. R., Feingold, G., & Moeng, C.-H. (1998). Large-eddy simulations of strongly precipitating, shallow, stratocumulus-topped boundary layers. *Journal of the Atmospheric Sciences*, *55*(24), 3616–3638. https://doi.org/10.1175/1520-0469(1998)055<3616:LESOSP>2.0.CO;2

Wood, R. (2012). Stratocumulus clouds. *Monthly Weather Review*, *140*(8), 2373–2423. https://doi.org/10.1175/MWR-D-11-00121.1

Wood, R., & Bretherton, C. S. (2004). Boundary layer depth, entrainment, and decoupling in the cloud-capped subtropical and tropical marine boundary layer. *Journal of Climate*, *17*(18), 3576–3588. https://doi.org/10.1175/1520-0442(2004)017<3576:BLDEAD>2.0.CO;2

Wood, R., & Hartmann, D. L. (2006). Spatial variability of liquid water path in marine low cloud: The importance of mesoscale cellular convection. *Journal of Climate*, *19*(9), 1748–1764. https://doi.org/10.1175/JCLI3702.1

Wood, R., Leon, D., Lebsock, M., Snider, J., & Clarke, A. D. (2012). Precipitation driving of droplet concentration variability in marine low clouds. *Journal of Geophysical Research*, *117*, D19210. https://doi.org/10.1029/2012JD018305

Wyant, M. C., Bretherton, C. S., Rand, H. A., & Stevens, D. E. (1997). Numerical simulations and a conceptual model of the stratocumulus to trade cumulus transition. *Journal of the Atmospheric Sciences*, *54*(1), 168–192. https://doi.org/10.1175/1520-0469(1997)054<0168:NSAACM>2.0.CO;2

Zheng, Y., Rosenfeld, D., & Li, Z. (2016). Quantifying cloud base updraft speeds of marine stratocumulus from cloud top radiative cooling. *Geophysical Research Letters*, *43*, 11,407–11,413. https://doi.org/10.1002/2016GL071185

Zheng, Y., Rosenfeld, D., & Li, Z. (2018). The relationships between cloud top radiative cooling rates, surface latent heat fluxes, and cloud-base heights in marine stratocumulus. *Journal of Geophysical Research: Atmospheres*, *123*. https://doi.org/10.1029/2018JD028579

Zhou, X., Kollias, P., & Lewis, E. R. (2015). Clouds, precipitation, and marine boundary layer structure during the MAGIC field campaign. *Journal of Climate*, *28*(6), 2420–2442. https://doi.org/10.1175/JCLI-D-14-00320.1

Zuidema, P., Painemal, D., De Szoeke, S., & Fairall, C. (2009). Stratocumulus cloud-top height estimates and their climatic implications. *Journal of Climate*, *22*(17), 4652–4666. https://doi.org/10.1175/2009JCLI2708.1